

## Application of Electron Bernstein Wave Heating and Current Drive to High $\beta$ Plasmas\*

P.C. Efthimion 1), G. Taylor 1), B. Jones 1), R.W. Harvey 4), A. K. Ram 3), P. Smirnov 5), T. Munsat 1), G. Bell 2), A. Bers 3), J. Decker 3), J.C. Hosea 1), R. Kaita 1), N. Lashmore-Davies 6), R. Majeski 1), D. A. Rasmussen 2), J. Spaleta 1), J. Wilgen 2), J. R. Wilson 1)

1) Princeton Plasma Physics Laboratory, Princeton, NJ, 08543, U.S.A.

2) Oak Ridge National Laboratory, Oak Ridge, TN, 37831, U.S.A.

3) Plasma Science and Fusion Center, M.I.T., Cambridge, MA, 02139, U.S.A.

4) CompX, Del Mar, CA, 92014, U.S.A.

5) Moscow State University, Moscow, Russia

6) Euratom - UKAEA Fusion Assoc., Culham Science Centre, Abingdon, Oxon, U K.

e-mail contact for main author: pefthimion@pppl.gov

**Abstract.** Electron Bernstein Waves (EBW) can potentially heat and drive current in high- $\beta$  plasmas. Electromagnetic waves can convert to EBW via two paths. O-mode heating, demonstrated on W-7AS, requires waves be launched within a narrow  $k$ -parallel range. Alternately, in high- $\beta$  plasmas, the X-mode cutoff and EBW conversion layers are millimeters apart, so the fast X-mode can tunnel to the EBW branch. We are studying the conversion of EBW to the X-mode by measuring the radiation temperature of the cyclotron emission and comparing it to the electron temperature. In addition, mode conversion has been studied with an approximate kinetic full-wave code. We have enhanced EBW mode conversion to  $\sim 100\%$  by encircling the antenna with a limiter that shortens the density scale length at the conversion layer in the scrape off of the CDX-U spherical torus (ST) plasma. Consequently, a limiter in front of a launch antenna achieves efficient X-mode coupling to EBW. Ray tracing and Fokker-Planck codes have been used to develop current drive scenarios in NSTX high- $\beta$  (10-40%) ST plasmas and a relativistic code will examine the potential synergy of EBW current drive with the bootstrap current.

### 1. Introduction

Steady state operation at high performance is a goal for many magnetic fusion plasma configurations. It is important for fusion reactors to have steady state operation demonstrated in next step experiments, such as ITER, FIRE, and a volumetric neutron source. These confinement devices rely on large currents to provide confinement and stability. For steady state operation, most of the total current will be bootstrap current because the power requirements for non-inductive current are prohibitively expensive. However, not all of the steady state current will be supplied by this means. Current profile control will be required to maximize stability and confinement. For low- $\beta$  plasmas, current profile control can be provided by ECCD. For high- $\beta$  plasmas, like the spherical torus (ST), electron Bernstein waves (EBWs) have the potential to heat and drive current. These waves propagate in the over-dense ( $\omega_{pe}/\omega_{ce} \gg 1$ ) regions of plasma while electromagnetic waves at low harmonics of the electron cyclotron frequency do not. In this paper we review the experimental studies of EBW in the CDX-U and NSTX ST's (Section 3). The mode conversion of EBW to the X-mode is examined by measuring the radiation temperature of the electron cyclotron emission and comparing it to the plasma electron temperature. Optimized mode conversion EBW heating and current drive experiments can be designed on the basis of the emission results. In section 2 we will review the EBW theory that relates the emission coefficients to the mode conversion excitation coefficients and justifies the study of EBW mode conversion for heating and current drive on the basis of the emission results [1,2]. In Section 4 we use the

---

\*This work was supported by DOE Contract No. DE-AC02-76-CHO-3073, DE-FG02-91ER-54109 and DE-FG02-99ER-54521, and by UK DTI, and EURATOM.

theory and experimental results to develop high- $\beta$  current drive scenarios for the NSTX ST. In addition, detailed modeling of EBW heating and current drive scenarios for NSTX equilibria with plasma  $\beta$ 's  $\sim 10 - 40\%$  have been conducted with the GENRAY EBW ray tracing code and the CQL3D bounce-averaged Fokker-Planck code. These scenarios are important first steps in defining EBW requirements for driving substantial currents in NSTX plasmas.

## 2. Theory

EBW mode conversion can occur via two processes. The first process involves conversion of EBWs to the fast X-mode [3-5]. EBWs first convert to the slow X-mode at the upper hybrid resonance layer (UHR). A cutoff-resonance-cutoff triplet formed by the left hand cutoff of the slow X-mode, the UHR, and the right hand cutoff of the fast X-mode allows the slow X-mode to tunnel through the UHR to the fast X-mode. This is the conversion process investigated on CDX-U and NSTX, and it is also being studied on the MST reversed-field pinch [6]. We will refer to this process as "B-X conversion". The mode conversion efficiency ( $C$ ) for  $k_{\parallel} = 0$  is given by [5]:

$$C = 4e^{-\pi\eta} \left(1 - e^{-\pi\eta}\right) \cos^2(\phi/2 + \theta) \quad (1)$$

where  $\cos^2(\phi/2 + \theta)$  is a phase factor relating to the phasing of the waves in the mode conversion region and the term preceding this is the maximum mode conversion efficiency. Here  $\eta$  is a tunneling parameter, which for magnetic scale lengths much greater than the density scale length at the UHR [5], is given by:

$$\eta \approx \left[ \omega_{ce} L_n (c\alpha) \right] \left[ (1 + \alpha^2)^{1/2} - 1 \right]^{1/2} \quad (2)$$

where  $L_n$ , the density scalelength, and  $\alpha = \omega_{pe} / \omega_{ce}$  are evaluated at the UHR layer and  $c$  is the velocity of light. From these equations it can be seen that the B-X conversion efficiency is very sensitive to changes in  $L_n$  at the UHR layer where the wave frequency,  $\omega = \omega_{UHR}$ . B-X mode conversion is particularly well suited for ST plasmas since the UHR layer for fundamental EBW conversion lies in the scrape off layer outside the last closed flux surface (LCFS) where  $L_n$  can be modified without affecting plasma performance. On CDX-U and NSTX the maximum mode conversion efficiency for fundamental EBWs occurs for  $L_n \sim 0.3 - 0.6$  cm. The second mode conversion process requires the coincidence of the X-mode and O-mode cutoffs [7-11]. This "B-X-O conversion", has been studied extensively on Wendelstein 7-AS both for heating [12] and as a  $T_e(R)$  emission diagnostic [13]. The B-X-O emission leaves the plasma through an angular window at an oblique angle with a transmission function given by [9,11]:

$$T(N_{\perp}, N_{\parallel}) = \exp \left\{ -\pi k_o L_n \sqrt{(Y/2)} \left[ 2(1 + Y)(N_{\parallel, opt} - N_{\parallel})^2 + N_{\perp}^2 \right] \right\} \quad (3)$$

where:  $k_o$  is the wavenumber,  $N_{\parallel, opt}^2 = [Y / (Y + 1)]$ ,  $Y = (\omega_{ce} / \omega)$ ,  $\omega_{ce}$  is evaluated at the cutoff and  $\omega$  is the wave frequency. For CDX-U and NSTX this B-X-O emission window is located at about  $35^\circ$  from the antenna axis. The emission window has a width that increases

with decreasing  $L_n$  at the O-mode cutoff. It can contribute to the measured X-mode emission if there is polarization scrambling of the O-mode emission resulting from reflections.

### General Relationships of Emission and Excitation Coefficients

An approximate full-wave kinetic model for the propagation of X- and O-modes, and the EBWs, in sheared magnetic field and in slab geometry, has been described in [2]. With the appropriate boundary conditions, this model is used to study the excitation of EBWs by externally launched X- or O-modes, and the emission of EBWs from inside the plasma. The emitted EBWs mode convert to X- and O-modes near the UHR and are subsequently observed in emission experiments. We find that the fraction of the X-mode (O-mode) energy flow that is mode converted to EBWs when an X- mode (O-mode) is launched from the low density side is the same as the emitted EBW energy flow that is mode converted to an X-mode (O-mode) that propagates out into the low density region [2,14]. These relationships arise from three fundamental properties that are satisfied by a set of loss-free mode conversion equations: linearity, energy flow conservation, and (Onsager-like) time reversibility [2,14]. On the basis of these equalities, the emission results from CDX-U and NSTX can be used for studying mode conversion excitation of EBWs for heating and current drive in ST plasmas.

### 3. EBW Emission Measurements on CDX-U and NSTX

Both CDX-U and NSTX are overdense beyond the LCFS on the outboard side. Second harmonic EBWs from the plasma core convert to X-mode near the LCFS and fundamental EBWs mode-convert between the LCFS and the vacuum vessel wall. Mode-converted fundamental and second harmonic EBW emission from NSTX and CDX-U was measured normal to the magnetic field with microwave radiometry. Radiometers operate in the 8-18 GHz band on NSTX and 4-12 GHz band on CDX-U [15]. The radiometers are calibrated absolutely with a Dicke-switched blackbody calibration source. On NSTX, dual-ridged antennas view the emission through a vacuum window and are oriented to accept, predominantly, X-mode polarized emission during the current flat top. On CDX-U, initial measurements were made with a similar arrangement, but later measurements used an in-vessel quad-ridged antenna that incorporates a local limiter and these will be discussed below.

The radial localization of the EBW emission source was confirmed on CDX-U by perturbing the  $T_e$  profile with a series of cold gas puffs, a technique used earlier by Laqua *et al.* [13]. The cold gas puffs locally cooled the plasma edge producing an inward propagating temperature response. The delay in the arrival time of the temperature pulse was found to be a maximum for EBWs emitted from the Shafranov-shifted magnetic axis at  $R=40$  cm. The delay versus radius in the plasma core is consistent with an electron diffusivity of  $3.2 \pm 2.2 \text{ m}^2\text{s}^{-1}$  [16]. This verification that the EBW emission source is localized at the ECE resonance justifies a comparison between the measured  $T_{rad}$  and Thomson scattering  $T_e$  profiles.

The natural steepening of the edge density gradient that occurs at the L to H transition can enhance the conversion and tunneling efficiency of both the B-X and B-X-O conversion processes if the steepening occurs in the vicinity of the EBW mode conversion layer. This has been observed for B-X-O conversion on MAST [17] and B-X conversion on NSTX [18]. In

NSTX plasmas with H-mode transitions the mode-converted EBW emission is observed to increase by up to a factor three at L to H transitions. The emission increase is coincident with steepening of the edge density profile during the H-mode.  $L_n$  data from Thomson scattering were used to calculate  $C$ . Good agreement was found between the measured EBW  $T_{rad}/T_e$  and the calculated  $C$  [19]. However, even during the H-mode phase the B-X conversion efficiency on NSTX is only 10-15%. Similarly, on CDX-U  $T_{rad}/T_e$  has been typically  $\leq 20\%$ .

Recently, experiments on NSTX have used the high harmonic fast wave (HHFW) antenna structure as a local limiter to steepen  $L_n$  in the B-X conversion region and hence improve the B-X conversion efficiency. An EBW radiometer and a microwave reflectometer that measures the density profile in the scrape-off were co-located near the midplane between two of the HHFW antenna straps. When the gap between the plasma edge and the HHFW antenna was reduced,  $L_n$  shortened from  $\sim 2.0$  cm to  $\sim 0.7$  cm and the EBW  $T_{rad}/T_e$  increased from 10% to 50%, in good agreement with theory [5]. Indeed, rather than relying on the  $L_n$  that occurs naturally, a local adjustable limiter could control and optimize  $L_n$  for maximum  $C$ .

### Experiments to Optimize B-X Conversion

An in-vacuum antenna/Langmuir probe assembly that can scan in major radius was installed on CDX-U [20]. In order to vary  $L_n$  for maximum mode conversion efficiency, the antenna/probe assembly is surrounded by a limiter, that can be positioned at different major radii relative to the antenna. Since B-X conversion of fundamental and second harmonic EBWs occurs in the scrape-off, this local limiter can be positioned to optimize the B-X conversion without perturbing the plasma. Four Langmuir probes continuously measure the density profile in front of the antenna. The antenna is a quad-ridged, broadband horn that can simultaneously measure O-mode and X-mode polarized emission. Data from the antenna/probe assembly show that  $L_n$  at the fundamental B-X conversion layer can be shortened from 3-6 cm to about 0.7 cm when the limiter is inserted in front of the antenna (Fig. 1). As a result, the B-X conversion efficiency, inferred from EBW  $T_{rad}/T_e$ , has been increased by an order of magnitude to  $\sim 100\%$ . Second harmonic conversion efficiency was also increased to  $\sim 100\%$  with the limiter in front of the antenna, although conversion efficiency was already  $\sim 70\%$  without the limiter, due to the steeper natural  $L_n$  closer to the LCFS.

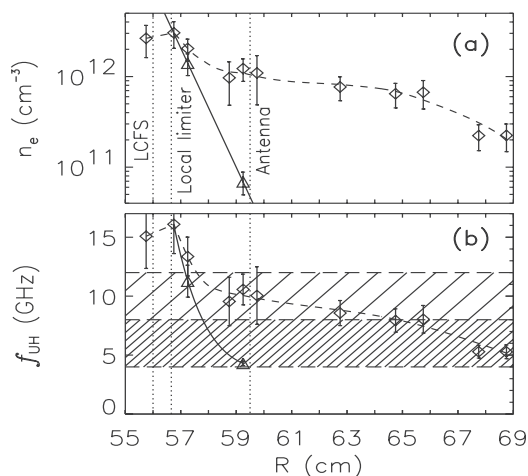


**Figure 1** (a)  $L_n = 3.6$  cm without a local limiter (dashed line and diamonds) was reduced to  $\sim 0.7$  cm with the local limiter inserted close to the LCFS (solid line and triangles). (b) UHR frequencies calculated for density profiles in (a). The two shaded regions show the frequency range of fundamental and second harmonic EBW emission.

The EBW emission is observed to fluctuate rapidly ( $\sim 10$  kHz) and is anti-correlated with the electron density fluctuation at the Langmuir probe closest to the B-X conversion layer. High

time resolution ( $\sim 1 \mu\text{s}$ ) electron density data, obtained simultaneously from the Langmuir probes, has allowed measurement of  $L_n$  fluctuations and the calculation of the fluctuations in  $C$ . While there is some correlation between fluctuations in  $C$  and the EBW  $T_{rad}$ , there are clearly EBW  $T_{rad}$  fluctuations that do not correlate. Refractive effects corresponding to MHD activity can contribute approximately half of the EBW  $T_{rad}$  fluctuations in CDX-U.

#### 4. NSTX EBW Heating and Current Drive

EBW heating and current drive are attractive for an ST plasma because they may provide local heating and driven currents that can help optimize the magnetic equilibrium and suppress MHD. EBW wave steering can take advantage of the relatively strong poloidal field and large magnetic shear.  $n_{||}$  shifts can result when EBWs are launched with  $n_{||}=0$  from a RF launcher poloidally displaced from the plasma mid-plane. Trapped particle effects on the low field side of the magnetic axis make deposition of EBW power on the high field side very attractive for current drive. However, there are three ranges of  $\beta$  that each present different challenges for high field side deposition. For plasmas with  $\beta \sim 10\%$ , the low aspect ratio of these ST plasmas makes access much beyond the axis problematic. At  $\beta \sim 20\%$  the mod B profile flattens around the axis significantly compromising localization of the heating and current drive. At  $\beta \sim 40\%$  a magnetic well forms near the axis making the mod B profile non-monotonic and complicating high field side access.

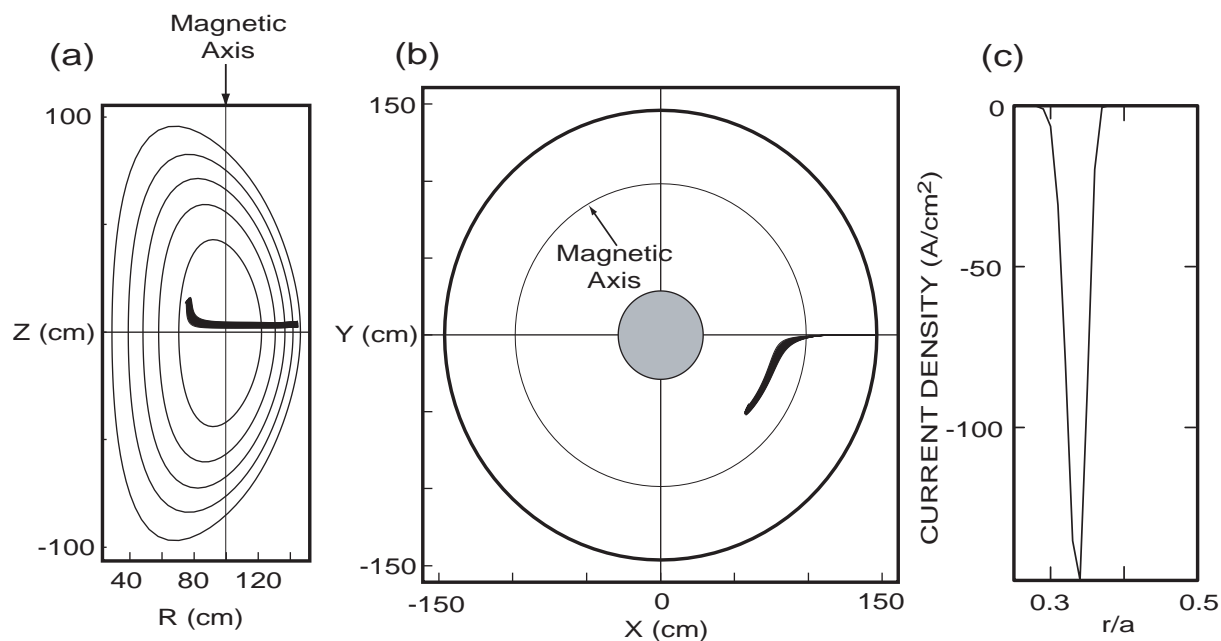


**Figure 2** (a) Poloidal and (b) toroidal cross sections of an NSTX  $\beta=20\%$ ,  $n_{eo}=3 \times 10^{19} \text{m}^{-3}$ ,  $T_{eo}=1 \text{keV}$  plasma showing path of 14.5 GHz EBW rays launched over a 10 cm poloidal length  $5^\circ$  above midplane, with  $-0.1 < n_{||} < 0.1$ . (c) Current drive localization for this case with 1 MW of EBW power.

Figure 2 shows the EBW ray trajectories calculated by the GENRAY ray tracing code [21] for 14.5 GHz EBWs launched  $5^\circ$  above the midplane into a standard  $\beta=20\%$  NSTX plasma. A bundle of rays are launched over a 10 cm poloidal length displaced  $5^\circ$  above the mid-plane with  $-0.1 < n_{||} < 0.1$ . Modeling of the current drive is performed with the CQL3D bounce-averaged Fokker-Planck code [22]. The current is very localized (Fig. 2c) on the inboard side and the efficiency is comparable to ECCD (0.065 A/W). A tight  $n_{||}$ -spectrum is necessary to avoid second harmonic damping and maintain a localized current deposition. The current localization is satisfactory for EBWs to stabilize neoclassical tearing modes that limit  $\beta$  for this plasma [23]. For a  $\beta=12\%$  a poloidal launch angle of  $10^\circ$ ,  $-0.25 < n_{||} < 0.25$ , and a launch

frequency of 12 GHz, the damping occurs at  $r/a = 0.3$  on the high field side. The efficiency is 0.08 A/W and is comparable to ECCD.

Future studies include an EBW launcher design that incorporates a local limiter to optimize the X-B tunneling and to broaden the O-X-B transmission window for EBW heating and current drive on NSTX. The X-B mode conversion scenarios will be examined by studying the physics of the B-X emission process. Currently, quad-ridged antennas with an adjustable limiter are being installed inside NSTX to view both B-X and B-X-O emissions. These emission measurements will guide the design of a high power ( $\sim 1$  MW) antenna for EBW heating and current drive on NSTX.

### References

- [1] EFTHIMION, P.C., et al., *Rev. Sci. Instrum.* **70**, 1018 (1999).
- [2] RAM, A.K., et al., *Phys. Plasmas* **9**, 409 (2002).
- [3] NAKAJIMA, S. and H. ABE, *Phys. Rev. A* **38**, 4373 (1988).
- [4] SUGAI, H., *Phys. Rev. Lett.* **47**, 1899 (1981).
- [5] RAM, A.K., and SCHULTZ, S. D., *Phys. of Plasmas* **7**, 4084 (2000).
- [6] CHATTOPADHYAY, P.K., et al., *Phys. Plasmas* **9**, 752 (2002).
- [7] PREINHAELTER, J. and KOPÉCKY, V., *J. Plasma Phys.* **10**, 1 (1973).
- [8] WEITZNER, H. and BATCHELOR, D.B., *Phys. Fluids* **22**, 1355 (1979).
- [9] MJØLHUS, E., *J. Plasma Phys.* **31**, 7 (1984).
- [10] NAKAJIMA, S. and ABE, H., *Phys. Lett. A* **124**, 295 (1987).
- [11] HANSEN, F.R., et al., *J. Plasma Phys.* **39**, 319 (1988).
- [12] LAQUA, H.P., et al., *Phys. Rev. Lett.* **78**, 3467 (1997).
- [13] LAQUA, H.P., et al., *Phys. Rev. Lett.* **81**, 2060 (1998).
- [14] BERS, A. and RAM, A.K., *Phys. Lett. A* **301**, 442 (2002).
- [15] TAYLOR, G., et al., *Rev. Sci. Instrum.* **72**, 285 (2001).
- [16] MUNSAT, T., et al., *Phys. Plasmas* **9**, 480 (2002).
- [17] AKERS, R.J., et al., *Phys. Rev. Lett.* **88**, 035002 (2002).
- [18] MAINGI, R., et al., *Phys. Rev. Lett.* **88**, 035003 (2002).
- [19] TAYLOR, G., et al., *Phys. Plasmas* **9**, 167 (2002).
- [20] JONES, B., et al. Princeton Plasma Physics Laboratory Report PPPL-3659 (January 2002).
- [21] SMIRNOV, A.P., and HARVEY, R.W., *Bull. Am. Phys. Soc.* **40**, 1837 (1995).
- [22] HARVEY, R.W., et al., *Proc. IAEA Tech. Com. on Advances in Simulation and Modeling of Thermonuclear Plasmas*, Montreal (IAEA, Vienna, 1993) p. 489.
- [23] GANTENBEIN, G., et al., *Phys. Rev. Lett.* **85**, 1242 (2000).